Efficiency at maximum power of a heat engine working with a two-level atomic system

Rui Wang,[1] Jianhui Wang,[1,2,*] Jizhou He,[1] and Yongli Ma[2]
[1]*Department of Physics, Nanchang University, Nanchang 330031, China*
[2]*State Key Laboratory of Surface Physics and Department of Physics, Fudan University, Shanghai 200433, China*
(Received 26 October 2012; revised manuscript received 27 February 2013; published 23 April 2013)

We consider the finite-time operation of a quantum heat engine whose working substance is composed of a two-level atomic system. The engine cycle, consisting of two quantum adiabatic and two quantum isochoric (constant-frequency) processes and working between two heat reservoirs at temperatures T_h and $T_c(<T_h)$, is a quantum version of the classical Otto cycle. By optimizing the power output with respect to two frequencies, we obtain the efficiency at maximum power output (EMP) and analyze numerically the effects of the times taken for two adiabatic and two isochoric processes on the EMP. In the absence of internally dissipative friction, we find that the EMP is bounded from the upper side by a function of the Carnot efficiency η_C, $\eta_+ = \eta_C^2/[\eta_C - (1-\eta_C)\ln(1-\eta_C)]$, with $\eta_C = 1 - T_c/T_h$. This analytic expression is confirmed by our exact numerical result and is identical to the one derived in an engine model based on a mesoscopic or macroscopic system. If the internal friction is included, we find that the EMP decreases as the friction coefficient increases.

DOI: 10.1103/PhysRevE.87.042119 PACS number(s): 05.70.−a, 03.65.−w

I. INTRODUCTION

Although the quasistatic Carnot cycle has the highest efficiency for engines working between two heat reservoirs at temperatures T_h and T_c $(<T_h)$, its power output vanishes because the time required for completing the cycle should be infinitely large. From a theoretical and a practical viewpoint, the engine cycle should be speeded up to obtain a finite power and the study of the efficiency at maximum power output (EMP) is thus deserved. Within the framework of finite-time thermodynamics, Curzon and Ahlborn introduced [1] the EMP for macroscopic heat engines, $\eta_{\rm CA} = 1 - \sqrt{\frac{T_c}{T_h}}$, which is known as Curzon-Ahlborn (CA) efficiency and, in fact, was obtained by Yvon [2] and Novikov [3] much earlier than by the authors of Ref. [1]. Up to now the entire issue of EMP has been ill-defined in at least two ways. First, the EMP is closely dependent on the variable with respect to which the maximization is implemented [4]. Second, a novel notion of efficiency first introduced in Ref. [5] has cast doubt on the entire issue: it seems to be unclear what sort of efficiency is sought if one departs from the ideal framework of Carnot. Despite some sort of universality of the CA efficiency revealed by several theoretical studies [6–10], it is still controversial in the following respects: (1) To the best of our knowledge, no experiments have been done to verify its validity. (2) The temperature differences between the working substance and the reservoirs are variables when maximizing the power, but they are not easily controllable [11]. (3) The time in the adiabatic phase is assumed to be proportional to the time in the isothermal phase. This assumption is not based on a strong physical argument and does not seem compelling. In practice, the EMP for any thermodynamic cycle working with two heat reservoirs depends sensitively on the temperatures of the reservoirs, the heat transfer law between the working substance and the heat reservoir, and irreversible losses as well as friction during the cycle. Different values for the EMP and various bounds of these values have been obtained for the macroscopic [6–8,11–20] and microscopic heat engines [9,10,21–24].

As in classical heat engines, there are various kinds of quantum heat engines [9,25–27], such as the Carnot engine [24,27–29], the Otto engine [19,20,22,30,31], the Brayton engine [29,32], the Stirling engine [33], etc. Except for the Carnot cycle, the performance of the engine cycles is dependent on the property of the working substance. Because of quantum features of the working substance, the thermodynamic observables in quantum heat engines are associated with the expectation of values of operators, and quantum equations of motion are used to describe the time evolution of the observables in quantum heat engines under finite-time operation [9,10,22,29,30]. Among all the studies about quantum heat engines, a central concern is to study the performance in finite time and the EMP in particular. To understand the relation between quantum mechanics and thermodynamics, a single-particle system has always been used as a heat engine [25–27] in which the cycle period is, however, infinitely long and the output power is vanishing. Rarely has the performance in finite time of a quantum heat engine working with a single-particle system been discussed. In view of the recent experimental realization of a microscopic heat engine [33], in which the working substance is a single particle in an optical trap, the analysis of the performance in finite time for a single-particle system as a heat engine would be expected to present significant implications in the experimental explorations of quantum features in small systems. Therefore, it is of great interest to consider the performance in finite time of a single-particle system as a heat engine.

In the present paper, a quantum Otto engine model is constructed by a two-level atomic system as its working substance. Based on an equation of motion, we derive the cycle period and the power output. We follow the traditional definition of the efficiency: the amount of energy input that is actually converted to useful output, and study the maximum power as well as its corresponding efficiency by optimizing with respect to two frequencies. The effects of the times taken for the adiabatic as well as the isochoric processes on the

*wangjianhui@ncu.edu.cn

EMP of the quantum Otto engine are analyzed numerically. We obtain the upper bound of the EMP for the frictionless engine: $\eta_+ = \eta_C^2/[\eta_C - (1-\eta_C)\ln(1-\eta_C)]$. This analytical expression is the same as the obtained one in the heat engine of the perfect Feymann's rachet [21] and of the classical particle transport [34]. If the internal friction in two adiabatic processes is considered, our result shows that the friction yields a decrease in the EMP.

II. A HEAT ENGINE MODEL OF A TWO-LEVEL ATOMIC SYSTEM

For a two-level atomic system [31,35], the energy spectrum can be expressed as $\varepsilon_\nu = \nu\hbar\omega$, where ω is the frequency and ν is the quantum number with $\nu = 1$ and 2. The system energy reads $E = \sum_\nu p_\nu \varepsilon_\nu$, with p_ν being the occupation probability of the νth eigenstate. Accordingly, the energy of a two-level system is given by

$$E = p_g\hbar\omega + 2p_e\hbar\omega, \tag{1}$$

where we have used $p_g \equiv p_1$ and $p_e \equiv p_2$. If the single-particle system is in thermal equilibrium with a heat reservoir at constant temperature T, the occupation probabilities p_g and p_e must satisfy the Boltzmann distribution $p_e = p_g e^{-\hbar\omega/k_BT}$, with k_B being the Boltzmann constant. It follows, using the constraint $p_e + p_g = 1$, that the occupation probabilities for the two states are obtained:

$$p_g = 1 - p_e = \frac{1}{e^{-\beta\omega}+1}, \tag{2}$$

where $\beta = 1/T$ denotes the inverse temperature of T. Here and in the following we set $\hbar = k_B = 1$ for simplicity. Substitution of Eq. (2) into Eq. (1) leads to

$$E = n\omega = \frac{2e^{-\beta\omega}+1}{e^{-\beta\omega}+1}\omega, \tag{3}$$

where $n = p_g + 2p_e$ has been used for the ratio $n = E/\omega$. The dynamics of the occupations at the ground and excited states, p_g and p_e, can be described via a master equation [10,23]:

$$\frac{dp_e}{dt} = -k_\downarrow p_e + k_\uparrow p_g, \quad \frac{dp_g}{dt} = -k_\uparrow p_g + k_\downarrow p_e, \tag{4}$$

where $k_\downarrow$ and $k_\uparrow$ denote the transition rates from the excited to the ground level and vice versa. Detailed balance introduces temperatures in the above explicit form of these coefficients. From Eq. (4), we can obtain the equation of motion for n,

$$\frac{dn}{dt} = -\gamma(n - n^{\rm eq}), \tag{5}$$

where $\gamma = k_\downarrow + k_\uparrow$ is the heat conductivity and $n^{\rm eq} = \frac{k_\downarrow + 2k_\uparrow}{k_\downarrow + k_\uparrow}$ is the asymptotic value of n. This asymptotic ratio must correspond to the value at thermal equilibrium: $n^{\rm eq} = \frac{2e^{-\beta\omega}+1}{e^{-\beta\omega}+1}$. Comparison of these two expressions for $n^{\rm eq}$ gives rise to the relation of detailed balance, $k_\uparrow/k_\downarrow = e^{-\beta\omega}$, which ensures that the system evolves in a specific way to the correct equilibrium state asymptotically [10].

III. QUANTUM OTTO CYCLE

The first law of thermodynamics in quantum-mechanical systems can be expressed as a function of eigenenergies ε_ν and occupation probabilities p_ν [26,28],

$$dE = đQ + đW = \sum_\nu \varepsilon_\nu dp_\nu + \sum_\nu p_\nu d\varepsilon_\nu, \tag{6}$$

where $đQ = \sum_\nu \varepsilon_\nu dp_\nu$ and $đW = \sum_\nu p_\nu d\varepsilon_\nu$ depict the heat exchange and work done, respectively. In an adiabatic process, there is no heat exchange ($đQ = 0$) as the occupation probabilities p_ν do not change, but work may still be nonzero (since eigenenergies ε_ν may change) according to Eq. (6).

The time for relaxation can be assumed to be zero for an adiabatic process of some microscopic or mesoscopic models [17,36] at the sudden limit. However, the time required for completing a classical and quantum adiabatic process should be large either in a macroscopic system or in most microscopic systems when the system volume or trap size changes very slowly. In general, the time scale of the change of the system state in a quantum adiabatic process must be much larger than that of the dynamical one, $\sim\hbar/E$ [24,28,31,37], so that the quantum adiabatic theorem [37] can apply. Otherwise, nonadiabatic dissipation (e.g., inner friction [10,22,24,30]) occurs and the quantum adiabatic condition is not fulfilled because of the rapid change in the energy level structure of the quantum system.

Equation (6), together with Eq. (3), gives rise to the relation

$$dE = đW + đQ = nd\omega + \omega dn, \tag{7}$$

where $đQ = \omega dn$ and $đW = nd\omega$. The energy of the system can change either by particle transition from one level to the other (changing n) or by varying the energy gap between the two levels (changing ω). It is clear that a thermodynamic process during which the ratio $n(\omega,T)$ remains constant is a quantum adiabatic process.

The quantum Otto cycle, consisting of two quantum adiabatic (fixed n) and two quantum isochoric processes (fixed ω), is illustrated in Fig. 1(a). The four thermodynamic processes that our engine model operates are described as follows.

(1) Isochoric process $1 \to 2$. The frequency ω_b is fixed and thus no work is done. The working subsystem is coupled to a heat reservoir at inverse temperature β_h for a period τ_h, with $\beta_h = 1/T_h$. Assuming that the irreversible entropy production is induced exclusively by the irreversibilities across finite differences of temperatures between the working system and the heat reservoir [38,39], we can directly use Eq. (7) to calculate the heat current as

$$\frac{đQ_h}{dt} = \omega_b\frac{dn(t)}{dt} = \gamma_h\left[n_h^{\rm eq} - n(t)\right]\omega_b, \tag{8}$$

where γ_h represents the heat conductivity between the working substance and the hot reservoir and $n_h^{\rm eq}$ is the ratio of the system at thermal equilibrium with the hot reservoir. Here $n(t)$ is required to satisfy the boundary conditions $n(0) = n_1(\omega_b,\beta_1)$ and $n(\infty) = n_h^{\rm eq}(\omega_b,\beta_h)$.

It is not very difficult to find the general solution of Eq. (5), $n(t) = n_h^{\rm eq} + (n_1 - n_h^{\rm eq})e^{-\gamma_h t}$, which leads to the relation

$$n_2 = n_h^{\rm eq} + \left(n_1 - n_h^{\rm eq}\right)x, \tag{9}$$

where $x = e^{-\gamma_h\tau_h}$. The heat transport from the hot reservoir in the isochoric process becomes

$$Q_h = E_2 - E_1 = (n_2 - n_1)\omega_b. \tag{10}$$

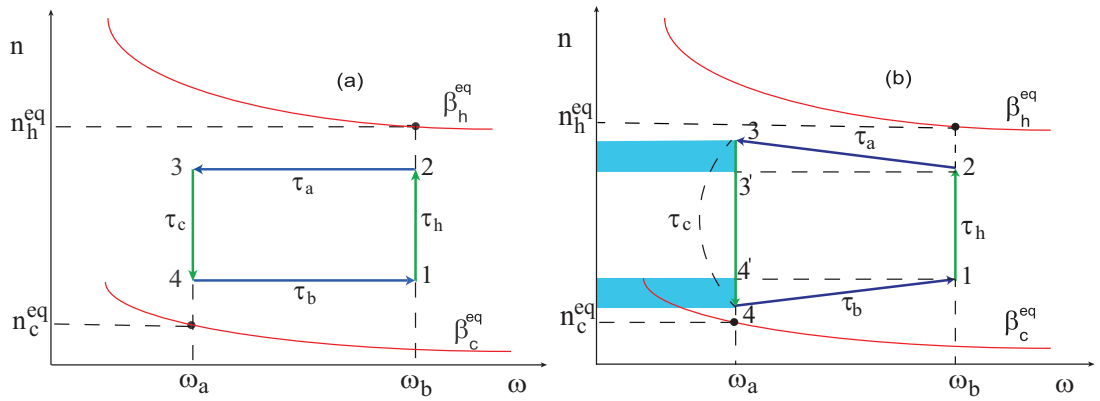

FIG. 1. (Color online) Schematic diagram of a quantum Otto cycle in the (ω,n) plane: (a) without internal friction and (b) with internal friction. $1 \to 2$ and $3 \to 4$ are two isochoric processes, while $2 \to 3$ and $4 \to 1$ are two adiabatic processes. n_h^{eq} and n_c^{eq} are two ratios of the atomic system at thermal equilibrium with two heat reservoirs at inverse temperatures β_h and β_c.

(2) Adiabatic expansion $2 \to 3$. The system decouples from the hot reservoir for a period τ_a when the frequency changes from ω_b to ω_a at a very slow speed in order for the quantum adiabatic condition [37] to be satisfied. To calculate the time taken for the adiabatic expansion and compression, we borrow directly from Refs. [22,31],

$$\tau_a = \tau_b = \alpha^{-1} \ln(\omega_b/\omega_a), \tag{11}$$

where α is a universal nonadiabatic parameter for a given system. Here τ_b is the time taken to complete the adiabatic compression, which is discussed in the following. No heat exchange between the system and its surroundings occurs but work is done by the system. According to Eq. (7), the work done on the system after this process can be calculated as

$$W_{23} = \int_{\omega_b}^{\omega_a} n d\omega = n_2(\omega_a - \omega_b), \tag{12}$$

where we have used $n_2 = n_3$. In order to realize the adiabatic process, the work will be produced by coupling the system with a work source (sink). This work source (sink) should be an external field like a radiation field [31]. Just through this external field the work either positive or negative will be done by the two-level system when we change the energy of the system.

(3) Isochoric process $3 \to 4$. The system is coupled to a cold reservoir at inverse temperature β_c $(>\beta_h)$ in a time of τ_c but no work is produced. As in the process $1 \to 2$, there are no irreversibilities except for the irreversibility due to the finite temperature difference between the system and the cold reservoir. Thus, the heat current during this process can be determined according to

$$\frac{d\!\!\!^{-}Q_c}{dt} = \omega_a \frac{dn(t)}{dt} = \gamma_c \left[n_c^{eq} - n(t)\right] \omega_a. \tag{13}$$

The relation between the distributions n_3 and n_4 at the initial and final states becomes

$$n_4 = n_c^{eq} + \left(n_3 - n_c^{eq}\right) y, \tag{14}$$

where $y = e^{-\gamma_c \tau_c}$. Here γ_c is the heat conductivity between the working substance and the cold reservoir and n_c^{eq} is the the ratio E^{eq}/ω of the single-particle system in thermal equilibrium with the cold reservoir. Here $n(t)$ must satisfy the boundary conditions: $n(0) = n_2(\omega_a,\beta_3)$ and $n(\infty) = n_c^{eq}(\omega_a,\beta_c)$. The heat absorbed by the system from the cold reservoir is given by

$$Q_c = E_4 - E_3 = (n_1 - n_2)\omega_a, \tag{15}$$

where the use of $n_1 = n_4$ and $n_2 = n_3$ has been made [see Fig. 1(a)].

(4) Adiabatic compression $4 \to 1$. The frequency ω is changed very slowly (as in the adiabatic expansion) to its initial value, while the ratio n is kept unchanged. The time required for completing this adiabat, τ_b, is given by Eq. (11). No heat is exchanged but the work is produced during the adiabatic process when the system is coupled to a work sink which also may be a radiation field as an external field. Similarly to the process $4 \to 1$, the work extracted from the work source is

$$W_{41} = \int_{\omega_a}^{\omega_b} n d\omega = n_1(\omega_b - \omega_a). \tag{16}$$

By repeatedly performing the above sequence of steps, heat as a form of energy is systematically extracted from the hot reservoir, some of which is released to the cold reservoir and the rest of which is delivered as work. After a single cycle, the total energy of the system as a state function remains unchanged, namely, $\Delta E = Q_h + Q_c + W_{23} + W_{41} = 0$. Thus, the total work done by the system per cycle, with $W = -(W_{23} + W_{41})$, and the efficiency are, respectively, given by

$$W = Q_h + Q_c = (n_2 - n_1)(\omega_b - \omega_a) \tag{17}$$

and

$$\eta = \frac{W}{Q_h} = 1 - \frac{\omega_a}{\omega_b}. \tag{18}$$

IV. THE EFFICIENCY AT MAXIMUM POWER OUTPUT

The combination of Eq. (14) with Eq. (9) gives rise to the following relations:

$$n_1 = n_c^{\rm eq} + \frac{(1-y)x}{1-xy}\Delta n^{\rm eq}, \quad n_2 = n_h^{\rm eq} - \frac{(1-x)y}{1-xy}\Delta n^{\rm eq}, \tag{19}$$

and

$$n_2 - n_1 = f(x,y)\Delta n^{\rm eq}, \tag{20}$$

where $f(x,y) = \frac{(1-x)(1-y)}{1-xy}$ and $\Delta n^{\rm eq} = n_h^{\rm eq} - n_c^{\rm eq}$, with

$$\Delta n^{\rm eq} = \frac{1}{e^{-\beta_c\omega_a}+1} - \frac{1}{e^{-\beta_h\omega_b}+1}. \tag{21}$$

The total work in Eq. (17) then becomes

$$W = f(x,y)(\omega_b - \omega_a)\Delta n^{\rm eq}. \tag{22}$$

It should be noted that the treatment adopted above to derive the expression of work, Eq. (22), in which the variables (times of two isochoric processes and frequencies) are separated, was first proposed in Ref. [10]. Defining $\tau \equiv \tau_h + \tau_c + \tau_a + \tau_b$, the power output can be given by

$$P = \frac{W}{\tau} = \frac{f(x,y)\Delta n^{\rm eq}(\omega_b - \omega_a)}{2\alpha^{-1}\ln(\omega_b/\omega_a) + \tau_h + \tau_c}, \tag{23}$$

where the use of Eq. (11) has been made. From Eq. (22), the positive work condition is obtained as

$$\frac{\omega_b}{\omega_a} < \frac{\beta_c}{\beta_h} = \frac{T_h}{T_c}. \tag{24}$$

Only when this condition is fulfilled can the positive work be extracted from the heat engine model. It is expected that the efficiency of the present engine is bounded from above the Carnot value, $\eta_C = 1 - \beta_h/\beta_c$.

While power output can be optimized with respect to two degrees of freedom (the two frequencies ω_a and ω_b), as happens in the models of the perfect ratchet [21] and the classical particle transport [34], the optimization on power output can proceed requiring only one degree of freedom (either ω_a or ω_b), as occurs in the approach adopted in Ref. [40]. In order to obtain the maximum power P in the global region, here we should consider two frequencies ω_a and ω_b as two degrees of freedom.

Based on Eqs. (23) and (18), the EMP for the cycle can only be solved numerically if τ_h, τ_c, γ_h, γ_c, and α are given. The EMP is closely dependent on the nonadiabatic coefficient α and the times required for completing the two isochoric processes (τ_h and τ_c). Figure 2(a) shows that the EMP increases with an increase in the nonadiabatic parameter α and approaches an upper bound η_+ (which is discussed in the following) when α becomes very large [41] with fixed τ_h and τ_c, while Fig. 2(b) demonstrates that for given α it increases with an increase in the time spent on the two isochoric processes (τ_h and τ_c) and tends to be the upper bound η_+. In addition, other calculations [42], which are not plotted in the figures, show that at fixed α (or τ_h as well as τ_c) the EMP tends to be zero when τ_h and τ_c are (or α is) small enough. Fig. 2, together with our calculations, indicates that the value of EMP, $\eta_{\rm mp}$, is situated between

$$0 \equiv \eta_- < \eta_{\rm mp} \leqslant \eta_+. \tag{25}$$

It should be noted that, according to Eqs. (11) and (18), the efficiency of the engine can be expressed as a function of the time for any adiabatic process, $\eta = 1 - e^{-\alpha\tau_a}$, where $\tau_a = \tau_b = \alpha^{-1}\ln(\omega_b/\omega_a)$. It is therefore expected that the increase either in the times for the two adiabatic processes (τ_a and τ_b) or in the times for the isochoric processes (τ_h and τ_c) yields an increase in the EMP.

Now we turn to the calculation of the upper bound of the EMP, η_+. If α in Eq. (23) is (or τ_h and τ_c are) large enough, the maximum power can be approximated by a simple form:

$$P = \frac{f(x,y)\Delta n^{\rm eq}(\omega_b - \omega_a)}{\tau_h + \tau_c}, \tag{26}$$

where two frequencies and the time allocations are separated from each other.

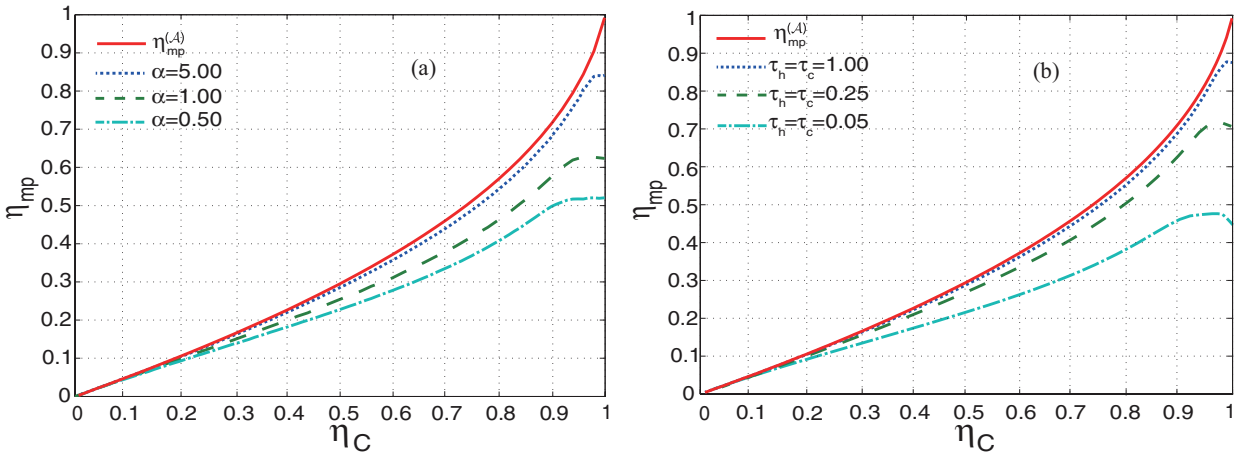

FIG. 2. (Color online) EMP, $\eta_{\rm mp}$, as a function of the Carnot efficiency η_C for (a) different values of α when $\tau_h = \tau_c = 0.69$ and (b) different values of τ_c and τ_h when $\alpha = 5.00$. The other parameters are taken as $\gamma_h = \gamma_c = 1.00$. $\eta_{\rm mp}^{(A)}$ given by Eq. (36) is denoted by a red solid line. The calculations of the EMP for (a) $\alpha = 5.00, 1.00$, and 0.50, and for (b) $\tau_h = \tau_c = 1.00$, 0.25, and 0.05, are represented by a blue dotted line, an olive dashed line, and a cyan dot-dashed line, respectively.

Setting the derivatives of P in Eq. (26) with respect to ω_a and ω_b equal to zero, we find the solution at

$$\frac{\beta_c\chi_c(\omega_b-\omega_a)}{\chi_c+1}=\frac{\chi_h-\chi_c}{\chi_h+1}, \tag{27}$$

$$\frac{\beta_h\chi_h(\omega_b-\omega_a)}{\chi_h+1}=\frac{\chi_h-\chi_c}{\chi_c+1}, \tag{28}$$

where $\chi_c=e^{-\omega_a\beta_c}$ and $\chi_h=e^{-\omega_b\beta_h}$. As a result, the value of ω_a/ω_b is

$$\frac{\omega_a}{\omega_b}=\frac{\beta_h}{\beta_c}\frac{\ln\chi_c}{\ln\chi_h}. \tag{29}$$

This equation presents the fundamental optimal relationship between ω_a and ω_b at maximum power output and can be done numerically. Using Eqs. (18) and (29), in Fig. 3 we plot the curve of the exact numerical value of EMP, $\eta_{\rm mp}^{(\mathcal{N})}$, versus the Carnot efficiency, η_C.

V. ANALYTIC EXPRESSION OF EFFICIENCY AT MAXIMUM POWER $\eta_{\rm mp}$

Dividing Eq. (28) by Eq. (27), we have $\sqrt{\frac{\beta_c\chi_c}{\beta_h\chi_h}}=\frac{\chi_c+1}{\chi_h+1}$, from which χ_h can be expressed as a function χ_c,

$$\chi_h=\frac{\left[1+2(1-r^2)\chi_c+\chi_c^2\right]-(1+\chi_c)\sqrt{\chi_c^2-(4r^2-2)\chi_c+1}}{2r^2\chi_c}, \tag{30}$$

where $r=\sqrt{\frac{\beta_c}{\beta_h}}$. We find, by multiplying Eqs. (27) and (28), $\omega_b-\omega_a=\frac{\chi_h-\chi_c}{\sqrt{\beta_c\beta_h\chi_c\chi_h}}$ and

$$\frac{\ln\chi_c}{\beta_c}-\frac{\ln\chi_h}{\beta_h}=\frac{\chi_h-\chi_c}{\sqrt{\chi_h\chi_c\beta_c\beta_h}}. \tag{31}$$

In order to derive an analytic result, we start our analysis by expanding χ_h in Eq. (30) up to the fourth order:

$$\chi_h=r^2\chi_c+(-2r^2+2r^4)\chi_c^2+(3r^2-8r^4+5r^6)\chi_c^3 +(-4r^2+20r^4-30r^6+14r^8)\chi_c^4+O\left(\chi_c^5\right). \tag{32}$$

From a mathematical point of view (see the details in the Appendix), Eq. (32) can be simplified as

$$\chi_h=r^2\chi_c. \tag{33}$$

As pointed out in the Appendix, the simple form [Eq. (33)] of Eq. (32) is valid, even in the case of the large relative difference of two heat reservoir temperatures (i.e., $r\gg1$ and $\eta_C=1-1/r^2$ approaches 1) and even in the low-temperature case when χ_c approaches 1. Combining Eqs. (31) and (33), we have

$$\ln\chi_c=-1-\frac{2\beta_c\ln r}{\beta_c-\beta_h},\qquad \ln\chi_h=\ln\chi_c+2\ln r. \tag{34}$$

The ratio of ω_a/ω_b in Eq. (29) is therefore

$$\frac{\omega_a}{\omega_b}=\frac{\ln\chi_c\beta_h}{\ln\chi_h\beta_c}=\frac{1}{r^2}\frac{1-r^2-2r^2\ln r}{1-r^2-2\ln r}. \tag{35}$$

In view of the fact that $r=1/\sqrt{1-\eta_C}$, with the Carnot efficiency $\eta_C=1-\beta_h/\beta_c$, the upper bound of EMP, η_+, can be expressed analytically as a function of η_C,

$$\eta_+\equiv\eta_{\rm mp}^{(\mathcal{A})}=\frac{\eta_C^2}{\eta_C-(1-\eta_C)\ln(1-\eta_C)}, \tag{36}$$

which is one main result of the present paper. If the time spent on two adiabatic processes is assumed to be proportional to the total cycle time or the total cycle time is given, the result [Eq. (36)] is rederived for the model, which can be envisioned as a model based on the particle transport in a quantum system. As emphasized, Eq. (36) derived from Eq. (33) for the quantum Otto engine is not only restricted to the classical limit when the temperatures are much greater than the frequencies, since Eq. (33) is valid even in the low-temperature case when the temperatures are much smaller than the frequencies and χ_c is approximately equal to 1.

Quite interestingly, this expression for the efficiency is identical to the one obtained for the engine model based on the perfect Feynman's ratchet (which is, in fact, the particle transport via Kramers' escape) [21] or the classical particle transport [34]. The EMP derived here is identical to the one derived for a model based on a mesoscopic [21] or macroscopic system [34], but it is valid in the region of all finite temperatures and thus not restricted to the high-temperature

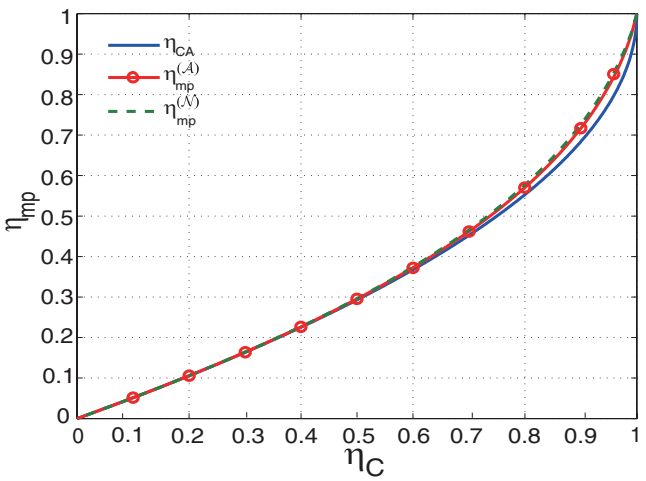

FIG. 3. (Color online) EMP, $\eta_{\rm mp}$, as a function of the Carnot efficiency, η_C. The numerical and analytic results of the efficiency, $\eta_{\rm mp}^{(\mathcal{N})}$ and $\eta_{\rm mp}^{(\mathcal{A})}$, are denoted by an olive dashed line and a red solid line with circles, respectively. The CA efficiency $\eta_{\rm CA}$ is represented by a blue solid line.

limit. Expanding $\eta_{\rm mp}^{(\mathcal{A})}$ up to the fourth term of η_C yields

$$\eta_{\rm mp}^{(\mathcal{A})} = \frac{\eta_C}{2} + \frac{\eta_C^2}{8} + \frac{7\eta_C^3}{96} + \frac{19\eta_C^4}{384} + O(\eta_C^5), \quad (37)$$

which is slightly larger than the expansion of the CA efficiency $\eta_{\rm CA}$, with $\eta_{\rm CA} = \frac{\eta_C}{2} + \frac{\eta_C^2}{8} + \frac{\eta_C^3}{16} + \frac{5\eta_C^4}{128} + O(\eta_C^5)$.

The analytic expression for the EMP $\eta_{\rm mp}^{(\mathcal{A})}$ is also plotted in Fig. 3, comparing the numerical result $\eta_{\rm mp}^{(\mathcal{N})}$ and the CA efficiency $\eta_{\rm CA}$. We see from Fig. 3 that the analytic result (red solid line with circles) is in nice agreement with the numerical value (olive dashed line) even for η_C up to 1.0, providing a strong argument in favor of our approach. The analytic and numerical results are slightly larger than the value of the CA efficiency η_{CA} (blue solid line). We also note that the present analytic and numerical results almost agree well with the CA efficiency even for η_C up to 0.6, at which the evident deviation of the present result from the CA efficiency starts to appear.

VI. AN ENGINE CYCLE WITH INTERNALLY DISSIPATIVE FRICTION

Up to now, we have only considered the ideal case that the irreversibility (e.g., internally dissipative friction) in any adiabatic process is ignored as the quantum adiabatic condition is satisfied. In practice, the two "adiabatic" processes of the heat engine cycle may be nonisentropic because of irreversible entropy production [18,24] when the quantum adiabatic condition is not fulfilled [see Fig. 1(b)]. When there exists nonadiabatic dissipation in an "adiabatic" process, the word adiabatic merely indicates that the working substance is isolated from a heat reservoir and no heat is exchanged between the system and its surroundings. Similarly to the the low-dissipation case [6,10,16,18,30], the increase of ratio n is assumed to be inversely proportional to the time required for completing the adiabatic process. That is, for the two adiabatic processes $2 \to 3$ and $4 \to 1$, we have

$$n_3 = n_2 + \Sigma_a/\tau_a, \quad n_1 = n_4 + \Sigma_b/\tau_b, \quad (38)$$

where Σ_a and Σ_b are friction coefficients for the two adiabatic processes. While the heat absorbed from the hot reservoir remains unchanged and is still given by Eq. (10), the (negative) heat extracted from the cold reservoir during the isochoric process, $Q_c = E_4 - E_3$, becomes

$$Q_c = \omega_a(n_1 - n_2) - \omega_a(\Sigma_a/\tau_a + \Sigma_b/\tau_b). \quad (39)$$

It follows that, using the same approach adopted in the frictionless engine cycle, the work is directly determined by

$$W = (n_2 - n_1)(\omega_b - \omega_a) - \omega_a(\Sigma_a/\tau_a + \Sigma_b/\tau_b). \quad (40)$$

On the right-hand side of Eq. (40), the first term represents the total positive work done by the system, while the second term is the total negative work done by the system [indicated by the two blue shaded areas in Fig. 1(b)] to overcome internal friction in two adiabats. From Eqs. (9), (14), and (38), we have

$$n_2 - n_1 = f(x,y)\Delta n^{\rm eq} - \frac{(1-x)(1/\tau_b - y/\tau_a)\Sigma}{1-xy}, \quad (41)$$

where $f(x,y)$ and $\Delta n^{\rm eq}$ were defined in Eq. (20). Here and hereafter we take $\Sigma = \Sigma_a = \Sigma_b$ for simplicity. The substitution of Eq. (41) into Eq. (40) leads to

$$W = f(x,y)\Delta n^{\rm eq}(\omega_b - \omega_a) - W_n, \quad (42)$$

with $W_n = \frac{\Sigma}{1-xy}[(1-x)\frac{\omega_b}{\tau_b} + (xy-y)\frac{\omega_b}{\tau_a} + (x-xy)\frac{\omega_a}{\tau_b} + (1+y-2xy)\frac{\omega_a}{\tau_a}]$ being the negative work done by the system to overcome the inner friction. From Eq. (42), we find the positive work ($W > 0$) condition,

$$\Delta n^{\rm eq} > \frac{W_n}{f(x,y)(\omega_b - \omega_a)}, \quad (43)$$

which must be fulfilled in order for positive work to be extracted from the engine. Substituting Eqs. (42) and (11) into the expressions of power and efficiency, $P = W/\tau$ and $\eta = W/Q_h$, we find

$$P = \frac{f(x,y)\Delta n^{\rm eq}(\omega_b - \omega_a)}{2\alpha^{-1}\ln(\omega_b/\omega_a) + \tau_h + \tau_c} - \frac{W_n}{2\alpha^{-1}\ln(\omega_b/\omega_a) + \tau_h + \tau_c} \quad (44)$$

and

$$\eta = 1 - \frac{\omega_a}{\omega_b} - \frac{2\alpha\Sigma}{f(x,y)\,[\Delta n^{\rm eq}\ln(\omega_b/\omega_a) - \alpha\Sigma]}\frac{\omega_a}{\omega_b}. \quad (45)$$

Based on Eqs. (44) and (45), one can present a numerical analysis of the EMP for the cycle if τ_h, τ_c, α, and Σ are given. The EMP depends sensitively on the friction coefficient Σ. Figure 4 shows that the EMP decreases with an increase in the friction coefficient Σ, as expected. When the inner friction is considered, the relative difference of two heat-reservoir temperatures, i.e., $(T_h - T_c)/T_h = \eta_C$, must be lager than the value η_Σ that is determined numerically and depends on Σ, such that the positive work condition (43) can be satisfied. For instance, we plot in the inset of Fig. 4 the lower bound of the relative temperature difference between two heat reservoirs, η_Σ, versus the friction coefficient, Σ. It is clear that η_Σ

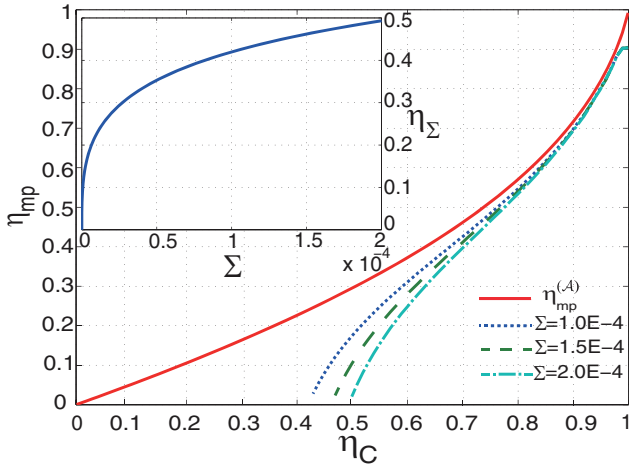

FIG. 4. (Color online) EMP, $\eta_{\rm mp}$, as a function of the Carnot efficiency, η_C, for different values of Σ when $\alpha = 10.00$. The other parameters are taken as $\gamma_h = \gamma_c = 1.00$ and $\tau_h = \tau_c = 0.69$. $\eta_{\rm mp}^{(\mathcal{A})}$ given by Eq. (36) is denoted by a red solid line. The calculations of the EMP for $\Sigma = 1.0 \times 10^{-4}$, 1.5×10^{-4}, and 2.0×10^{-4} are represented by a blue dotted line, an olive dashed line, and a cyan dot-dashed line, respectively. Inset: The lower bound of the relative temperature difference between two heat reservoirs, η_Σ, versus the friction coefficient, Σ, when $\alpha = 10.00$ is adopted.

decreases as the friction coefficient Σ decreases and tends to be zero when Σ approaches zero.

VII. CONCLUSION

In conclusion, we have focused on the study of the EMP of a two-level atomic system as a heat engine model. We obtained the EMP of the engine model by optimizing the power output with both the frequencies. We have found that the EMP increases with increasing the times either for the two adiabatic processes or for the two isochoric processes and is bounded between $0 < \eta_{\rm mp} \leqslant \eta_+$, where the upper bound of the EMP, η_+, is analytically derived in the form of Eq. (36). This value of the EMP, confirmed by our exact numerical result, is the same as that in a simple model working with a mesoscopic or macroscopic system. In the presence of the internal friction, we proved that the EMP for the engine cycle with internal friction (without a fixed cycle time) decreases with an increase in the value of the friction coefficient Σ.

Throughout the paper, the notation of the EMP as an idealized objective is not well-defined and not necessarily physically. Perhaps more fundamental notations of the EMP (such as the sustainable efficiency [5]) can be adopted to study the performance in finite time of the quantum Otte cycle in future.

ACKNOWLEDGMENTS

This work is supported by the National Natural Science Foundation of China under Grants No. 11265010, No. 11147200, No. 11065008, No. 10974033, and No. 11191240252; the State Key Programs of China under Grant No. 2012CB921604; and the Foundation of Jiangxi Educational Committee under Grant No. GJJ12136. J.W. is very grateful to Professor Zhanchun Tu at Beijing Normal University and Dr. Huiyi Tang at Fudan University for useful discussions.

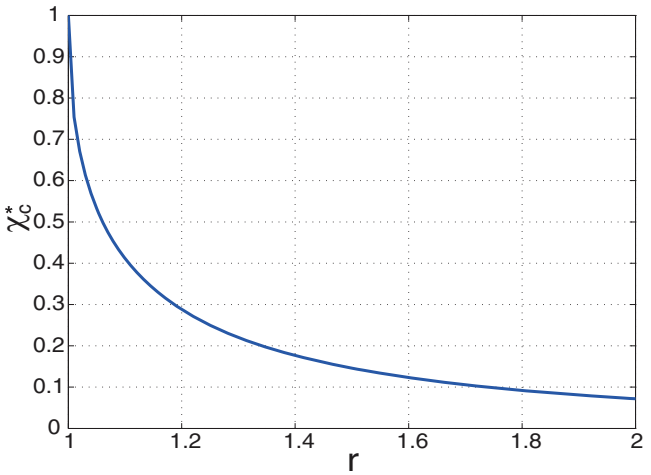

FIG. 5. (Color online) The upper bound of χ_c as a function of the ratio r.

APPENDIX: THE REASON WHY χ_h CAN BE APPROXIMATED BY $\chi_h = r^2\chi_c$

The value of χ_c in Eq. (30) must fulfill the condition $\chi_c^2 - (4r^2 - 2)\chi_c + 1 > 0$ in order for χ_h to be a real number. Combining this condition with the fact that $0 < \chi_c < 1$, we find χ_c should be bounded between $0 < \chi_c \leqslant \chi_c^*$, where $\chi_c^* = -1 + 2r^2 - \sqrt{-1 + (-1 + 2r^2)^2}$ is the upper bound of χ_c. As the temperature ratio r increases, χ_c^* decreases quickly and becomes much smaller than 1 (see Fig. 5). On the one hand, when r is obviously larger than 1, the value of χ_c becomes very small in comparison with 1, i.e., $\chi_c \ll 1$. On the other hand, if r is approximated equal to 1, the expansion coefficients on the right side of Eq. (32) tend to be zero. Based on the two above facts, Eq. (32) can thus simplify to Eq. (33), which is not restricted to the regime of small relative difference of two heat reservoir temperatures [16] with $r \approx 1$ and the high-temperature limit when the temperatures are much greater than the frequencies with $\chi_c \ll 1$.

[1] F. Curzon and B. Ahlborn, Am. J. Phys. **43**, 22 (1975).
[2] J. Yvon, in *Proceedings of the International Conference on Peaceful Uses of Atomic Energy* (United Nations Publications, Geneva, 1955), Vol. 2, p. 387.
[3] I. I. Novikov, J. Nucl. Energy II **7**, 125 (1958).
[4] B. Gaveau, M. Moreau, and L. S. Schulman, Phys. Rev. E **82**, 051109 (2010); M. Moreau, B. Gaveau, and L. S. Schulman, *ibid.* **85**, 021129 (2012).
[5] B. Gaveau, M. Moreau, and L. S. Schulman, Phys. Rev. Lett. **105**, 060601 (2010).
[6] M. Esposito, R. Kawai, K. Lindenberg, and C. Van den Broeck, Phys. Rev. Lett. **105**, 150603 (2010), and references therein.
[7] Y. Izumida and K. Okuda, Eur. Phys. J. B **77**, 499 (2010).
[8] Y. Apertet, H. Ouerdane, C. Goupil, and Ph. Lecoeur, Phys. Rev. E **85**, 041144 (2012).
[9] E. Geva and R. Kosloff, J. Chem. Phys. **96**, 3054 (1992); **97**, 4396 (1992).
[10] T. Feldmann and R. Kosloff, Phys. Rev. E **61**, 4774 (2000).
[11] Y. Izumida and K. Okuda, Europhys. Lett. **83**, 60003 (2008); **97**, 10004 (2012).
[12] C. Van den Broeck, Phys. Rev. Lett. **95**, 190602 (2005).
[13] J. C. Guo, J. Y. Wang, Y. Wang, and J. C. Chen, Phys. Rev. E **87**, 012133 (2013).
[14] J. C. Chen, J. Phys. D: Appl. Phys. **27**, 1144 (1994); L. Chen and Z. Yan, J. Chem. Phys. **90**, 3740 (1989).
[15] Z. C. Tu, Chin. Phys. B **21**, 020513 (2012).
[16] Y. Wang and Z. C. Tu, Europhys. Lett. **98**, 40001 (2012); Phys. Rev. E **85**, 011127 (2012); Commun. Theor. Phys. **59**, 175 (2013).
[17] T. Schmiedl and U. Seifert, Europhys. Lett. **81**, 20003 (2008).
[18] J. H. Wang and J. Z. He, Phys. Rev. E **86**, 051112 (2012).
[19] X. L. Huang, T. Wang, and X. X. Yi, Phys. Rev. E **86**, 051105 (2012).
[20] O. Abah, J. Roßnagel, G. Jacob, S. Deffner, F. Schmidt-Kaler, K. Singer, and E. Lutz, Phys. Rev. Lett. **109**, 203006 (2012).

[21] Z. C. Tu, J. Phys. A: Math. Theor. **41**, 312003 (2008).
[22] Y. Rezek and R. Kosloff, New J. Phys. **8**, 83 (2006).
[23] B. Rutten, M. Esposito, and B. Cleuren, Phys. Rev. B **80**, 235122 (2009).
[24] J. H. Wang, J. Z. He, and Z. Q. Wu, Phys. Rev. E **85**, 031145 (2012).
[25] H. T. Quan, Y. X. Liu, C. P. Sun, and F. Nori, Phys. Rev. E **76**, 031105 (2007).
[26] H. T. Quan, Phys. Rev. E **79**, 041129 (2009).
[27] C. M. Bender, D. C. Brody, and B. K. Meister, J. Phys. A: Math. Gen. **33**, 4427 (2000).
[28] R. Wang, J. H. Wang, J. Z. He, and Y. L. Ma, Phys. Rev. E **86**, 021133 (2012); J. H. Wang, J. Z. He, and X. He, *ibid.* **84**, 041127 (2011); J. H. Wang and J. Z. He, J. Appl. Phys. **11**, 043505 (2012).
[29] F. Wu, L. G. Chen, S. Wu, F. R. Sun, and C. Wu, J. Chem. Phys. **124**, 214702 (2006); J. Appl. Phys. **99**, 054904 (2006).
[30] J. H. Wang, J. Z. He, and Y. Xin, Phys. Scr. **75**, 227 (2007).
[31] J. H. Wang, Z. Q. Wu, and J. Z. He, Phys. Rev. E **85**, 041148 (2012).
[32] X. L. Huang, L. C. Wang, and X. X. Yi, Phys. Rev. E **87**, 012144 (2013).
[33] V. Blickle and C. Bechinger, Nat. Phys. **8**, 143 (2012).
[34] C. Van den Broeck and K. Lindenberg, Phys. Rev. E **86**, 041144 (2012).
[35] A two-level atomic system is in analogy with a single particle in a harmonic trap or a single-mode radiation field in a cavity under the assumption that only two energy levels are considered, and also with a spin-1/2 system.
[36] M. Esposito, K. Lindenberg, and C. Van den Broeck, Europhys. Lett. **85**, 60010 (2009); M. Esposito, R. Kawai, K. Lindenberg, and C. Van den Broeck, Phys. Rev. E **81**, 041106 (2010).
[37] M. Born and V. Fock, Z. Phys. **51**, 165 (1928).
[38] G. P. Beretta, Eur. Phys. Lett. **99**, 20005 (2012).
[39] H. Y. Tang, J. H. Wang, and Y. L. Ma (unpublished).
[40] S. Velasco, J. M. M. Roco, A. Medina, and A. C. Hernández, J. Phys. D: Appl. Phys. **34**, 1000 (2001).
[41] For instance, the EMP almost collapses into the the value of $\eta_{\rm mp}^{(\mathcal{A})}$ for α (or $\tau_h = \tau_c$) up to 10.0 (or 11.0), with $\gamma_h = \gamma_c = 1.0$ and $\tau_h = \tau_c = 0.69$ (or $\alpha = 5.0$), as indicated in Fig. 2. That is, in such a case the EMP for the present engine model approaches its upper bound, $\eta_+ = \eta_{\rm mp}^{(\mathcal{A})}$.
[42] As an example, our numerical calculations show that the EMP is almost vanishing and thus achieves its lower bound when α (or $\tau_h = \tau_c$) is reduced to about 1.0×10^{-4} (or 1.0×10^{-5}), with $\gamma_h = \gamma_c = 1.0$ and $\tau_h = \tau_c = 0.69$ (or $\alpha = 5.0$).